Comparison of classical, new corrected-classical, and semiclassical IR spectra of non-rotating H2O with quantum calculations

3 AUTHORS:

Alexey L Kaledin
Emory University
50 PUBLICATIONS **885** CITATIONS

SEE PROFILE

Xinchuan Huang
SETI Institute
85 PUBLICATIONS **2,105** CITATIONS

SEE PROFILE

Joel M Bowman
Emory University
541 PUBLICATIONS **15,093** CITATIONS

SEE PROFILE

Comparison of classical, new corrected-classical, and semiclassical IR spectra of non-rotating H_2O with quantum calculations

Alexey L. Kaledin *, Xinchuan Huang, Joel M. Bowman

Department of Chemistry and Cherry L. Emerson Center for Scientific Computing, Emory University, 1515 Dickey Drive, Atlanta, GA 30322, USA

Abstract

Model infrared spectra for non-rotating H_2O are calculated at 0 K, based on exact quantum, standard classical and semiclassical calculations. An accurate potential energy surface is used along with a realistic dipole function. An analysis of the classical and quantum spectrum in the harmonic approximation is presented at 0 K. This clearly reveals that the magnitude of the classical intensities is essentially arbitrary, depending on the total energy. Thus, the intensity of classical harmonic spectrum disagrees with the corresponding quantum one. A very simple correction to the classical spectrum is suggested that largely restores agreement with the harmonic quantum spectrum. A second, more general classical correction is also suggested, which, however, requires knowledge of the normal modes.
© 2003 Published by Elsevier B.V.

1. Introduction

The classical Molecular Dynamics approach to the calculation of infrared spectra [1] is well-known and widespread, especially in applications to large systems and/or condensed phases, where quantum approaches are prohibitively difficult to implement.

The expression for the IR spectrum of a system in thermal equilibrium in particular is given both classically and quantum mechanically (in first-order perturbation theory in the field–matter interaction) by [2]

$$I(\omega) = \frac{Re}{\pi} \int_0^\infty \mathrm{d}t\, \mathrm{e}^{-\mathrm{i}\omega t} \langle \mathbf{d}(t) \cdot \mathbf{d}(0) \rangle, \tag{1.1}$$

where $\langle \mathbf{d}(t) \cdot \mathbf{d}(0) \rangle$ is the average of the dipole auto-correlation function. Usually this averaging refers to a canonical distribution; however, it can also refer to a microcanonical average. This kind of averaging is the one of interest here.

There have been several suggestions made in the literature to correct the classical IR spectrum for a canonical distribution by noting the differences between the classical and quantum spectra in the (double) harmonic approximation. For an oscillator of frequency ω the correction factor of interest here is given by the ratio of the quantum and classical harmonic vibrational partition functions [1],

$$Q_{CM}(T) = \frac{k_B T}{\hbar \omega}, \tag{1.2a}$$

$$Q_{QM}(T) = \left[1 - \exp\left(-\frac{\hbar \omega}{k_B T} \right) \right]^{-1}. \tag{1.2b}$$

Obviously, this correction factor applies to a thermal averaged spectrum. It is also worth noting that the derivation of it assumes a linear approximation to the dipole moment function.

Here, we consider two corrections to the classical spectrum that are still based on the harmonic normal mode model; however, for a microcanonical ensemble, and where we consider a more general form for the dipole moment. We also present a numerical comparison of the model IR spectrum using exact quantum, several semiclassical and classical methods. We begin with brief description of these methods followed by results.

* Corresponding author. Fax: +1-4047276628.
E-mail address: akaledin@uclink.berkeley.edu (A.L. Kaledin).

2. Methods and calculation details

In this section, we give the details of the methods mentioned in Section 1 and discuss their performance on a realistic potential [3] and dipole moment surface [4] of the water molecule. To our knowledge, no rigorous comparison of this nature exists in the literature.

2.1. Classical and corrected classical

The classical Hamiltonian in mass-scaled normal coordinates is

$$H = \frac{1}{2} \sum_i \left[P_i^2 + \omega_i^2 Q_i^2 \right], \tag{2.1}$$

and the time-dependence of the coordinate and momentum of each normal mode is given by

$$Q_i(t) = Q_i(0) \cos(\omega_i t), \tag{2.2a}$$

$$P_i(t) = -Q_i(0) \sin(\omega_i t), \tag{2.2b}$$

where ω_i is the harmonic frequency of normal mode i. As usual, we begin by assuming the linear approximation for the dipole moment in the small-amplitude limit (about equilibrium), i.e.,

$$d_\alpha(t) = d_{e,\alpha} + \sum_i d_{e,\alpha,i} Q_i(t); \quad \alpha = x, y, z, \tag{2.3}$$

where the summation is over normal modes, and for simplicity we denote the dipole derivative in mode i by $d_{e,\alpha,i}$. Thus, the classical absorption spectrum, denoted $I_{CM}(\omega)$, is given by

$$I_{CM}(\omega) = \sum_i d_{e,\alpha,i}^2 \frac{\langle Q_i^2(0) \rangle}{2} \delta(\omega - \omega_i). \tag{2.4}$$

Note we have made use of the fact that $\langle Q_i(0) \rangle$ is zero for the harmonic oscillator, and thus cross terms involving $\langle Q_i(0) \rangle$ and mode–mode cross terms $\langle Q_i(0) Q_j(0) \rangle$ vanish. We have also shortened the notation by implying the summation of the final result over the three Cartesian components of the dipole operator.

For a microcanonical average,

$$\langle Q_i^2(0) \rangle = \frac{E_i}{\omega_i^2}, \tag{2.5}$$

where E_i is the total energy of mode i. Thus,

$$I_{CM}(\omega) = \sum_i d_{e,\alpha,i}^2 \frac{E_i}{2\omega_i^2} \delta(\omega - \omega_i). \tag{2.6}$$

Assuming E is the total energy, then E_i is just E/N, for N normal modes. Since E is arbitrary Eq. (2.6) cannot agree with the quantum result, which we review next.

Consider transitions from the ground vibrational state, in which case the quantum spectrum is given by

$$I_{QM}(\omega) = \sum_i d_{e,\alpha,i}^2 |\langle i|Q_i|0\rangle|^2 \delta(\omega - \omega_i) \tag{2.7a}$$

$$= \sum_i d_{e,\alpha,i}^2 \frac{\hbar}{2\omega_i} \delta(\omega - \omega_i). \tag{2.7b}$$

Comparing (2.7b) to the classical expression, Eq. (2.6), we see a similarity, and in fact equality if E_i equals $\hbar\omega_i$, the energy of the quantum transition. This choice of E_i does give a correction to the classical spectrum and while we are exploring using it, it clearly has a major drawback. The total energy of a molecule could be quite large if the energy in each mode is that of $\hbar\omega_i$, and, as is well-known, this energy could and almost certainly would 'leak' from mode to mode and lead to large deviations from the small amplitude limit (see, however, below). Another suggestion is to continue to use an arbitrary, but small value of E and hence a small value of E_i, and to multiply the resulting $I_{CM}(\omega)$ by ω/E_i. Assuming, as we have, that E_i equals E/N, the corrected-classical spectrum, denoted $I_{CCM}(\omega)$, is then given by

$$I_{CCM}(\omega) \equiv I_{CM} \frac{\hbar\omega N}{E}. \tag{2.8}$$

(Note this result is roughly related to the correction in the thermal case, which in the limit $k_B T/\hbar\omega \to 0$ is just $\hbar\omega/k_B T$.)

To gain insight into combination bands we continue to treat the motion as harmonic but consider the quadratic terms in the expansion of the dipole moment. The quantum spectrum is then given by

$$I_{QM}(\omega)$$
$$= \sum_{ij} \left| d_{e,\alpha,i,j} \langle i|Q_i|0\rangle \langle j|Q_j|0\rangle \right|^2 \delta[\omega - (\omega_i + \omega_j)] \tag{2.9a}$$

$$= \sum_{ij} d_{e,\alpha,i,j}^2 \frac{\hbar^2}{4\omega_i\omega_j} \delta[\omega - (\omega_i + \omega_j)], \tag{2.9b}$$

where $d_{i,j}$ is the matrix of second derivatives with respect to Q. The corresponding (uncorrected) classical spectrum is (ignoring the difference frequency term)

$$I_{CM}(\omega) = \sum_{ij} d_{e,\alpha,i,j}^2 \frac{E_i E_j}{4\omega_i^2 \omega_j^2} \delta[\omega - (\omega_i + \omega_j)]. \tag{2.10}$$

As before if we set E_i and E_j equal to $\hbar\omega_i$ and $\hbar\omega_j$, respectively, the classical and quantum spectra would agree. For the same reasons given before, this is not suggested. Instead the suggested correction for combination bands (and for fundamentals as well) is the following. Instead of using E_i equal to $\hbar\omega_i$ for normal mode i we suggest using a scaled energy $\alpha\hbar\omega_i$ for each normal mode, where $\alpha < 1$. In this case, the classical intensity for the fundamental and combination bands would differ from the correct quantum expression by the known factor α^2. By choosing α small the classical dynamics would be harmonic and correct intensities

should be straightforward to obtain. This procedure is somewhat more involved than simply multiplying the classical spectrum by ω, which is the correction for the fundamentals, since it requires knowledge of the normal modes.

In the present calculations, the classical spectrum was obtained in the usual way [1]. Twenty trajectories were propagated starting at the global minimum on the potential, with initial kinetic energy of 50 cm^{-1}. The velocity vectors were randomly distributed in the three vibrational modes, and classical equations of motion were solved. The phase space is further sampled during the $\sim$30 ps of total running time by applying a time averaging procedure [5],

$$I_{\text{CM}}(\omega) = \frac{1}{2\pi} \lim_{T\to\infty} \frac{1}{T} \left\langle \left| \int_0^T \mathrm{d}t\, d_\alpha(t)\, \mathrm{e}^{-\mathrm{i}\omega t} \right|^2 \right\rangle, \qquad (2.11)$$

where both the Fourier transform variable and the time averaging variable are allowed to run independently from 0 to T. Note the similarity between the above expression and the semiclassical expression appearing later in Eq. (2.18). In both formulas, averaging over time is utilized to facilitate the convergence of the phase space integral $\langle \cdots \rangle$.

2.2. Semiclassical-IVR

A consistent improvement over an MD simulation may be obtained by a semiclassical (SC) approximation of the time evolution operator, $\exp[-\mathrm{i}\hat{H}t/\hbar]$. In particular, the initial value representation theory (IVR) [6] has proven to be an accurate and practical method for capturing the essential quantum mechanical effects [7–10], such as coherence and superposition of amplitudes (interference). One needs to carry out the integration of a time dependent quantity over the initial positions and momenta of classical trajectories. An advantage of SC-IVR is that the formulation is completely general, i.e., it is very easy to extend it to large molecules.

Generally, a spectral density can be evaluated as a Fourier transform of an auto correlation function with respect to an arbitrary reference state. In the specific case of an IR spectrum, the reference state is chosen as the ground vibrational state operated on by the dipole moment,

$$I_{\mu\mu}^{\text{SC}}(E) = \frac{Re}{\pi\hbar} \int_0^\infty \mathrm{d}t\, \mathrm{e}^{\mathrm{i}Et/\hbar} \left\langle \Psi_g \hat{\mu} | \mathrm{e}^{-\mathrm{i}\hat{H}t/\hbar} | \hat{\mu} \Psi_g \right\rangle, \qquad (2.12)$$

where E is the energy of the system (including the zero point energy). We now apply the Herman–Kluk [11] IVR expression for the time evolution operator in F dimensions,

$$\mathrm{e}^{-\mathrm{i}\hat{H}t/\hbar} = \frac{1}{(2\pi\hbar)^F} \int \mathrm{d}\mathbf{p}_0$$
$$\times \int \mathrm{d}\mathbf{q}_0\, C_t(\mathbf{p}_0, \mathbf{q}_0)\, \mathrm{e}^{\mathrm{i}S_t(\mathbf{p}_0,\mathbf{q}_0)/\hbar} |\mathbf{p}_t\mathbf{q}_t\rangle\langle\mathbf{p}_0\mathbf{q}_0| \qquad (2.13)$$

and substitute it into Eq. (2.12)

$$I_{\mu\mu}^{\text{SC}}(E) = \frac{1}{(2\pi\hbar)^F} \frac{Re}{\pi\hbar} \int_0^\infty \mathrm{d}t\, \mathrm{e}^{\mathrm{i}Et/\hbar}$$
$$\times \int \mathrm{d}\mathbf{p}_0 \int \mathrm{d}\mathbf{q}_0\, C_t(\mathbf{p}_0, \mathbf{q}_0)\, \mathrm{e}^{\mathrm{i}S_t(\mathbf{p}_0,\mathbf{q}_0)/\hbar}$$
$$\times \langle \Psi_g \hat{\mu} | \mathbf{p}_t\mathbf{q}_t \rangle \langle \mathbf{p}_0\mathbf{q}_0 | \hat{\mu} \Psi_g \rangle, \qquad (2.14)$$

where the action integral is

$$S_t(\mathbf{p}_0, \mathbf{q}_0) = \int_0^t \mathrm{d}t'\, \left[p_{t'}^2(\mathbf{p}_0, \mathbf{q}_0) - H(\mathbf{p}_0, \mathbf{q}_0) \right], \qquad (2.15)$$

and $H(\mathbf{p}_0, \mathbf{q}_0)$ is the classical Hamiltonian. The Herman–Kluk prefactor C_t is a quantity that depends on the derivatives of the positions and momenta at time t with respect to those at time $t = 0$,

$$C_t(\mathbf{p}_0, \mathbf{q}_0) = \frac{1}{2^{F/2}} \left| \gamma^{1/2} \frac{\partial \mathbf{q}_t}{\partial \mathbf{q}_0} \gamma^{-(1/2)} + \gamma^{-(1/2)} \frac{\partial \mathbf{p}_t}{\partial \mathbf{p}_0} \gamma^{1/2} \right.$$
$$\left. - \mathrm{i}\gamma^{1/2} \frac{\partial \mathbf{q}_t}{\partial \mathbf{p}_0} \gamma^{1/2} + \mathrm{i}\gamma^{-(1/2)} \frac{\partial \mathbf{p}_t}{\partial \mathbf{q}_0} \gamma^{-(1/2)} \right|^{1/2}. \qquad (2.16)$$

The wavefunction for the coherent state [12,13] basis is given by a Gaussian multiplied by a complex plane wave,

$$\langle \mathbf{q} | \mathbf{p}_t\mathbf{q}_t \rangle = \left(\frac{\gamma}{\pi} \right)^{F/4} \mathrm{e}^{-(\gamma/2)(\mathbf{q}-\mathbf{q}_t)^2 + \mathrm{i}\mathbf{p}_t\cdot(\mathbf{q}-\mathbf{q}_t)} \qquad (2.17)$$

with γ being a diagonal matrix of Gaussian width parameters.

Following an earlier work on time averaging the HK-IVR expression for the spectral density [14], we use a simplified, approximate, expression for $I(E)$,

$$I_{\mu\mu}^{\text{SC}}(E) = \frac{(2\pi\hbar)^{-F}}{2\pi\hbar T} \int \mathrm{d}\mathbf{p}_0$$
$$\times \int \mathrm{d}\mathbf{q}_0 \left| \int_0^T \mathrm{d}t \langle \Psi_g \hat{\mu} | \mathbf{p}_t\mathbf{q}_t \rangle\, \mathrm{e}^{\mathrm{i}[Et+S_t(\mathbf{p}_0,\mathbf{q}_0)+\phi_t(\mathbf{p}_0,\mathbf{q}_0)]/\hbar} \right|^2, \qquad (2.18)$$

where the quantity ϕ_t is the phase of the prefactor C_t. The above form of the phase space average is much easier to converge while it retains all the important quantum effects embedded in the original expression (Eq. (2.14)). It can be further shown that even a single trajectory, if chosen carefully, is capable of reproducing the spectral density with reasonable accuracy [14]. For the calculations of bound state eigenvalues, it is convenient to start the trajectory at the potential minimum with the initial momentum in each normal mode k being $p_0^{(k)} = \sqrt{\omega_k}$, so that the total energy of the trajectory equals the harmonic zero point energy. We refer to such a calculation as SC-1.

The final elements in the calculation are the ground state wavefunction and the dipole moment. The time overlap integral appearing in Eq. (2.18) needs to be known analytically, and this limits our flexibility in choosing a suitable ground state wavefunction. Typically, the normal mode wavefunction, which is a product of one dimensional harmonic oscillator wavefunctions, is used in combination with a series expansion of the dipole moment function (usually to first or second order in coordinate). In the present calculations we also used the harmonic approximation for Ψ_g and the linear approximation to the dipole,

$$\langle \mathbf{q}|\Psi_g\rangle = \left(\frac{\gamma}{\pi}\right)^{F/4} e^{-(\gamma/2)(\mathbf{q}-\mathbf{q}_i)^2}, \tag{2.19a}$$

$$\mu_\alpha(\mathbf{q}) \simeq \mu_\alpha(\mathbf{q}_i) + \mu'_\alpha(\mathbf{q}_i)\cdot(\mathbf{q}-\mathbf{q}_i), \tag{2.19b}$$

where the Gaussian center $\mathbf{q}_i$ is the geometry at the global minimum on the potential, and $\mu'_\alpha(\mathbf{q}_i)$ is the α Cartesian component of the dipole first derivative vector at $\mathbf{q}_i$. Since the constant dipole $\mu_\alpha(\mathbf{q}_i)$ does not contribute to the absorption intensity, we only retain the linear term for practical calculations. Numerical simulations of phase space integral (2.18) were performed using Monte Carlo sampling. Trajectories are selected randomly and propagated for ~120 fs. For the sampling density we used the Husimi distribution function [15] at $t = 0$,

$$\left|\langle\Psi_g|\mathbf{p}_0\mathbf{q}_0\rangle\right|^2 = e^{-(\gamma/2)(\mathbf{q}_0-\mathbf{q}_i)^2} e^{-(1/2\gamma)(\mathbf{p}_0-\mathbf{p}_i)^2}. \tag{2.20}$$

Convergence was monitored by doubling the number of trajectories (starting with 125) and was reached after three steps, i.e., at 500 trajectories.

Next, consider the simpler, linearized SC-IVR approach. This is derived by first re-writing the quantum mechanical correlation function (appearing as Fourier transformed quantity in Eq. (2.12)) in the trace form,

$$C_{\mu\mu}(t) = \text{tr}\left[|\Psi_g\rangle\langle\Psi_g|\hat{\mu}e^{i\hat{H}t/\hbar}\hat{\mu}e^{-i\hat{H}t/\hbar}\right], \tag{2.21a}$$

where the quantum mechanical Boltzmann operator $e^{-\beta\hat{H}}$ at $T = 0$ K has been reduced to the projection operator onto the ground vibrational state. We can define operators $\hat{A}$ and $\hat{B}$ (given below) such that,

$$C_{\mu\mu}(t) = \text{tr}\left[\hat{A}e^{i\hat{H}t/\hbar}\hat{B}e^{-i\hat{H}t/\hbar}\right]. \tag{2.21b}$$

If one were to apply an IVR expression to each of the two time evolution operators, one would have two phase space averages, namely $(\mathbf{p}_0, \mathbf{q}_0)$ and $(\mathbf{p}_{0'}, \mathbf{q}_{0'})$. Referring to the work of Sun and Miller [16] on the 'linearized' model of SC-IVR, one can obtain the following expression for the correlation function,

$$C_{\mu\mu}^{\text{LSC}}(t) = (2\pi\hbar)^{-F}$$
$$\times \int d\mathbf{p}_0 \int d\mathbf{q}_0\, A^{\text{w}}(\mathbf{p}_0,\mathbf{q}_0)B^{\text{w}}(\mathbf{p}_t,\mathbf{q}_t)^*, \tag{2.22}$$

where A^{w} and B^{w} are the Wigner transforms [17] of these operators generally defined as,

$$A^{\text{w}}(\mathbf{p},\mathbf{q}) = \int d\mathbf{q}'\, e^{-i\mathbf{p}\cdot\mathbf{q}'}\left\langle \mathbf{q}+\frac{1}{2}\mathbf{q}'|\hat{A}|\mathbf{q}-\frac{1}{2}\mathbf{q}'\right\rangle. \tag{2.23}$$

Note the simplification of the phase space integrand of the Wigner model compared to the HK-IVR of Eq. (2.14). Both the classical action and the pre-exponential factor have been dropped and substituted by much smoother functions, i.e., Wigner transforms (in this case of the dipole moment operator). Performing the integration in Eq. (2.23) and dropping the constant dipole term $\mu_\alpha(\mathbf{q}_i)$ yields the following functions,

$$A^{\text{w}}(\mathbf{p}_0,\mathbf{q}_0) = 2\mu'_\alpha(\mathbf{q}_i)\cdot\left(\mathbf{q}_0-\mathbf{q}_i+\frac{i}{\gamma}\mathbf{p}_0\right)e^{-\gamma(\mathbf{q}_0-\mathbf{q}_i)^2}e^{-(1/\gamma)\mathbf{p}_0^2},$$
$$\tag{2.24a}$$

$$B^{\text{w}}(\mathbf{p}_t,\mathbf{q}_t) = \mu'_\alpha(\mathbf{q}_i)\cdot(\mathbf{q}_t-\mathbf{q}_i). \tag{2.24b}$$

The final expression for the correlation function in terms of the linearized (or Wigner) model becomes,

$$C_{\mu\mu}^{\text{LSC}}(t) = \frac{2}{(2\pi\hbar)^F}\int d\mathbf{p}_0 \int d\mathbf{q}_0\, e^{(-\gamma(\mathbf{q}_0-\mathbf{q}_i)^2-(1/\gamma)\mathbf{p}_0^2)}\mu'_\alpha(\mathbf{q}_i)$$
$$\times \left(\mathbf{q}_0-\mathbf{q}_i+\frac{i}{\gamma}\mathbf{p}_0\right)\mu'_\alpha(\mathbf{q}_i)\cdot(\mathbf{q}_t-\mathbf{q}_i), \tag{2.25}$$

and the spectrum is evaluated as a Fourier transform,

$$I_{\mu\mu}^{\text{LSC}}(\omega) = \frac{Re}{\pi\hbar}\int_0^\infty dt\, e^{-i\omega t}C_{\mu\mu}^{\text{LSC}}(t). \tag{2.26}$$

Similar to the previous case, the integration of Eq. (2.25) was done via Monte Carlo sampling using the Gaussian distribution function appearing in the integrand. The trajectories were propagated for ~600 fs, and the correlation function was converged with 2500 trajectories.

2.3. Quantum

The quantum calculations were done with the code MULTIMODE. This is a general code to perform quantum ro-vibrational energy calculations of polyatomic molecules. The code is based on the full Watson Hamiltonian for ro-vibrational motion, given in terms of mass-scaled normal modes, Q_i [18,19]. It has been described and tested previously [20–23]. A key feature of MULTIMODE is the representation of the full N-mode potential by a hierarchical series of mode-coupling terms. In the present calculations of three modes, the series is exact at the three-mode representation,

$$V(Q_1,Q_2,Q_3) = \sum_i V_i^{(1)}(Q_i) + \sum_{i>j} V_{ij}^{(2)}(Q_i,Q_j)$$
$$+ V_{123}^{(3)}(Q_1,Q_2,Q_3). \tag{2.27}$$

Eigenvalues and eigenfunctions of the Watson Hamiltonian were obtained using the following approach.

After solving a vibrational self-consistent field (VSCF) Hamiltonian for the ground vibrational state, the 'virtual' orthonormal basis of computed eigenfunctions were utilized in CI method, denoted VCI.

The potential minimum was chosen as the reference geometry in VSCF and VCI calculation. The numbers of HEG points used in numerical integrations are 22, 30 and 30 for Mode 1 (v_b), Mode 2 (v_{ss}) and Mode 3 (v_{as}), respectively. The vibrational wavefunctions were saved for later calculations. The direct results from MULTI-MODE calculations are the 'exact' intensities,

$$I(\omega_{i,j}) = |\langle \Psi_i | \hat{\mu} | \Psi_j \rangle|^2, \tag{2.28}$$

where ω_{ij} is the corresponding frequency for the transition between vibrational level i and j; $\hat{\mu}$ is the dipole moment operator, and Ψ_i and Ψ_j are molecular eigenstates.

3. Results and conclusions

Peak positions and relative intensities of the three H_2O vibrational modes are summarized in Table 1. The quantum results are treated as 'exact' ones. Such comparisons are only limited to 0 K $J = 0$ vibrational transition intensities and should not be used for comparison with previous experimental ratios. First, note that the quantum (double) harmonic results are in fair agreement with exact quantum ones for the line positions, but in very good agreement for the line intensities. This indicates that the linear approximation for the dipole moment is fairly accurate for the fundamentals of this strongly bound molecule, as expected. Of all the semiclassical and classical results, the SC-IVR results are overall in the best agreement with exact quantum ones for both the position and the intensities. The relative intensities and the positions of the two peaks are predicted very well. However, the weak v_b-band is not resolved in the SC-IVR spectrum. Fig. 1 superposes the QM result (a stick spectrum) and the SC-IVR calculation (Eq. (2.18)).

The (uncorrected) classical results are in excellent agreement with the quantum harmonic ones in the positions, but not in the intensities, as expected, based on
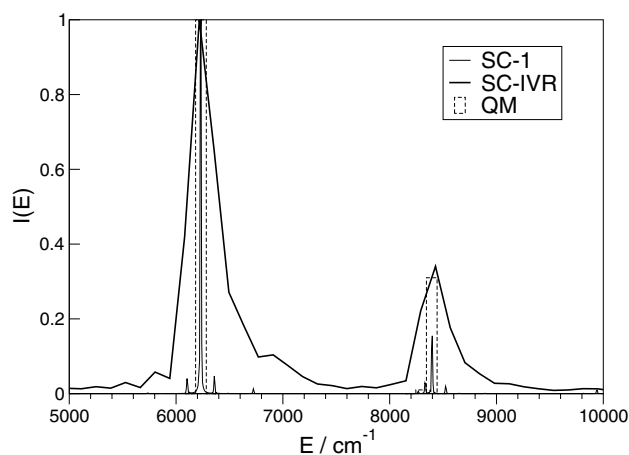

Fig. 1. The comparison of the IR spectrum from QM (dashed bar), SC-IVR (thick line) and a 'one trajectory' SC-1 (thin line) calculations.

the remarks in Section 2. The corrected CM intensities are in good agreement with the quantum harmonic ones, as they should be, and in this case also in good agreement with exact QM intensities. We also add the result from the SC-IVR calculation obtained with only one trajectory averaged over a much longer length of time.
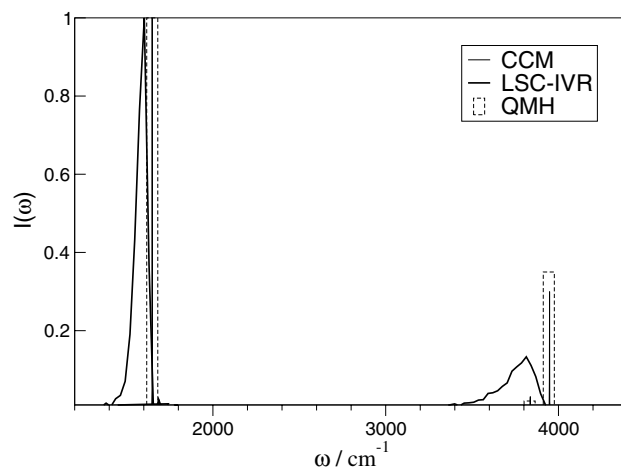

Fig. 2. The LSC-IVR calculation (thick line), the corrected-classical calculation CCM (thin line) and the quantum harmonic QMH result (dashed bar) for the IR spectrum.

Table 1
Relative intensities (first line) and peak positions in cm^{-1} (second line) of H_2O computed at various levels of theory

	QM	SC-IVR	SC-1	LSC-IVR	CM	CCM	QMH
$I(\omega_b)$	1.00	1.00	1.00	1.00	1.00	1.00	1.00
	1595	1580	1590	1615	1649	1649	1649
$I(\omega_{ss})$	0.01	–	–	–	0.02	0.05	0.02
	3657	–	–	–	3837	3837	3833
$I(\omega_{as})$	0.31	0.36	0.16	0.17	0.14	0.33	0.35
	3756	3791	3760	3865	3949	3949	3944

The information for $I(\omega_{ss})$ in the SC methods is missing due to the low resolution and extremely weak intensity.

Note that the SC-1 results are in good agreement with the quantum line positions, but interestingly the intensity is close to the uncorrected CM result. The most computationally efficient semiclassical method, the LSC-IVR, is significantly in better agreement with the exact line positions than the CM or CCM results, but the intensity is much closer to the CM than the correct QM one. This suggests that the simple correction to the CM would also correct the LSC spectrum. In Fig. 2, we show the LSC-IVR calculation (Eq. (2.22)) the corrected-classical CCM calculation and the quantum harmonic QMH calculation. The LSC-IVR method gives much improved peak positions from the harmonic limit, but similarly to SC-1 it lacks in accuracy for the relative intensity of v_{as}. Obviously, these two approximations, although both derived from the semiclassical IVR expression, cannot properly describe the quantum effects, unlike the full SC-IVR. However, it appears that the classical 'ω-correction' may also be applicable to the approximate formulations of semiclassical methods.

Acknowledgements

References

[1] P.H. Berens, K.R. Wilson, J. Chem. Phys. 74 (1981) 4872.
[2] R.G. Gordon, Adv. Magn. Reson. 3 (1968) 1.
[3] H. Partridge, D.W. Schwenke, J. Chem. Phys. 106 (1997) 4618.
[4] W. Gabriel, E.-A. Reinsch, P. Rosmus, S. Carter, N. Handy, J. Chem. Phys. 99 (1993) 897.
[5] D.W. Noid, M.L. Koszykowski, R.A. Marcus, J. Chem. Phys. 67 (1977) 404.
[6] W.H. Miller, J. Chem. Phys. 53 (1970) 3578.
[7] W.H. Miller, Faraday Discuss. 110 (1998) 1.
[8] D.J. Tannor, S. Garashchuk, Annu. Rev. Phys. Chem. 51 (2000) 553.
[9] E. Jezek, N. Makri, J. Phys. Chem. 105 (2001) 2851.
[10] W.H. Miller, J. Phys. Chem. 105 (2001) 2942.
[11] M. Herman, E. Kluk, Chem. Phys. 91 (1984) 27.
[12] E.J. Heller, J. Chem. Phys. 62 (1975) 1544.
[13] E.J. Heller, Acc. Chem. Res. 14 (1981) 368.
[14] A.L. Kaledin, W.H. Miller, J. Chem. Phys. 118 (2003) 7174.
[15] K. Husimi, Proc. Phys. Math. Soc. Jpn. 22 (1940) 264.
[16] X. Sun, W.H. Miller, J. Chem. Phys. 106 (1997) 916.
[17] E. Wigner, Phys. Rev. 40 (1932) 749.
[18] J.K.G. Watson, Mol. Phys. 15 (1968) 479.
[19] J.K.G. Watson, Mol. Phys. 19 (1970) 465.
[20] S. Carter, J.M. Bowman, N.C. Handy, Theor. Chim. Acta 100 (1998) 191.
[21] S. Carter, J.M. Bowman, J. Chem. Phys. 108 (1998) 4379.
[22] S. Carter, S.J. Culik, J.M. Bowman, J. Chem. Phys. 107 (1997) 10458.
[23] MULTIMODE (online documents and a more extensive list of references can be found at www.emory.edu/CHEMISTRY/faculty/bowman/multimode).